Colloids and Surfaces B: Biointerfaces xxx (2015) xxx–xxx

Contents lists available at ScienceDirect

Colloids and Surfaces B: Biointerfaces

journal homepage: www.elsevier.com/locate/colsurfb

Linoleic acid binding properties of ovalbumin nanoparticles

Osvaldo E. Sponton[a,b], Adrián A. Perez[a,b], Carlos R. Carrara[b], Liliana G. Santiago[b,*]

[a] Consejo Nacional de Investigaciones Científicas y Técnicas de la República Argentina (CONICET), 1 de Mayo 3250, 3000 Santa Fe, Argentina
[b] Instituto de Tecnología de Alimentos (ITA), Facultad de Ingeniería Química (FIQ), Universidad Nacional del Litoral (UNL), 1 de Mayo 3250, 3000 Santa Fe, Argentina

ARTICLE INFO

Article history:
Received 23 December 2014
Accepted 21 January 2015
Available online xxx

Keywords:
Ovalbumin
Nanoparticles
Linoleic acid
Fluorescence
Binding ability

ABSTRACT

In the present work, ovalbumin (OVA) solutions (10 g/L, 50 mM NaCl, pH 7.5) were heat-treated at 75, 80 and 85 °C (namely, OVA-75, OVA-80 and OVA-85, respectively), from 0 to 25 min. OVA nanoparticles (OVA_n) around 100 nm were obtained. For 3 min of heat treatment, OVA_n sizes increased with temperature, but for a heating time longer than 10 min, OVA-75 showed the highest size values. OVA_n surface hydrophobicity increased 6–8 folds in comparison with native OVA and wavelength blue shifts of 25–30 nm in maximum fluorescence intensity were registered. These results suggest that buried hydrophobic residues were exposed to the aqueous medium. Binding experiments with linoleic acid (LA) as polyunsaturated fatty acid (PUFA) model were carried out. Firstly, binding ability of OVA_n was determined from LA titration curves of intrinsic fluorescence measurements. OVA-85 at 5 min presented the highest binding ability and it was used for further binding properties studies (turbidity, particle size distribution – PSD – analysis and ζ-potential measurements). Turbidity measurement and PSD analysis showed that OVA_n–LA nanocomplexes were formed, avoiding LA supramolecular self-assembly formation. The union of LA to OVA_n surface confers them significant lower ζ-potential and larger size. Hence, fluorescence and ζ-potential results showed that LA would bind to OVA_n by mean of hydrophobic interactions. Information derived from this work could be important to potentially use OVA_n as PUFA vehiculization with applications in several industrial sectors (food, pharmaceutical, cosmetics, *etc.*).

1. Introduction

Egg white proteins (EWP) are extensively used in food industry due to their functional (foaming, gelling, emulsifying) and nutritional properties [1]. The main protein of egg white is ovalbumin (OVA) which represents 54% of EWP [2]. Therefore, OVA would be the main responsible of their functional properties [3]. OVA is a globular protein of 43 kDa molecular weight. It is formed for 385 aminoacids, of which a half are hydrophobic and a third are charged mainly acid, giving to the protein a pI ∼ 4.5 [4]. Furthermore, OVA has four sulfhydryl groups (SH) buried in the interior of its structure and one disulfide bridge (SS). SH groups can be superficially exposed as a consequence of heat-induced protein unfolding. Hence, SH can react *via* SH/SS interchange reactions. These ones are in part responsible of OVA aggregation under heating [4]. Moreover, heating produces exposition of buried hydrophobic groups producing aggregates with greater surface hydrophobicity than native OVA and so promoting aggregation by mean of hydrophobic interactions [4,5]. Conditions under which heating is made determine size and morphology of heat-treated OVA aggregates [1]. Nyemb et al. [1] found four distinct morphologies (linear, linear-branched, spherical and spherical-agglomerated) and sizes when OVA was heated at 80 °C under different pH and ionic strength conditions.

In general, denaturation and aggregation are required for several EWP applications. As it was mentioned, heating causes conformational changes which affect the folded structure promoting denaturation and then protein aggregation. These conformational changes can also be promoted by other process, such as enzymatic cleavage, high pressure, *etc.* [6,7]. Heat-induced OVA aggregation has been extensively studied in order to achieve a better understanding of denaturation/aggregation process and the changes in protein functional properties [1,4,6–8]. One of protein functional properties that have gained interest in the last years is the protein ability to bind hydrophobic or hydrophilic ligands, mainly bioactive compounds. In this sense, β-lactoglobulin and their aggregates are the most studied systems for the development of nanovehicles for bioactive compounds [9–13]. However, there are not many studies about the application of OVA for bioactive compounds vehiculization. It has been demonstrated that OVA has the ability

* Corresponding author. Tel.: +54 342 4571252x2602.
E-mail address: lsanti@fiq.unl.edu.ar (L.G. Santiago).

http://dx.doi.org/10.1016/j.colsurfb.2015.01.037
0927-7765/

to bind hydrophilic compounds such as caffeine, theophylline and diprophylline, forming complexes [14]. Furthermore, OVA also could bind hydrophobic compounds (*e.g.* stearic acid), which was characterized by a decrease in OVA intrinsic fluorescence [15]. Nevertheless, more studies are required in order to characterize the kind of interactions, in particular the interaction between OVA and polyunsaturated fatty acids, which has not been extensively evaluated yet.

Complexes obtained by the interaction protein–ligand can be applied in food and pharmaceutical industries for the following reasons: (i) protection of fatty acids (polyunsaturated) through its entrapment and immobilization in nanoscopic particles which prevent contact with prooxidant agents (enzymes, oxygen, light, metals) [9]; (ii) protein can improve water solubility of hydrophobic compound allowing their incorporation in clear food systems, such as certain beverages [9,16] and (iii) some protein–fatty acids (oleic, linoleic) complexes can present antitumor activity [17]. Moreover, these structures can be produced from food-grade compounds such as lipids, proteins and polysaccharides, which could allow their incorporation in foods [18].

Taking into account that there is a lack of studies about OVA-polyunsaturated fatty acid complex formation and that controlled heat treatment of OVA can generates nanostructures with a greater surface hydrophobicity [4], the ability of native and heat-induced OVA aggregates to bind linoleic acid was evaluated in the present work. Linoleic acid (LA) was taken as a model polyunsaturated fatty acid (PUFA). Information derived from this work could be of practical interest for the development of PUFAs vehiculization systems.

2. Materials and methods

2.1. Materials

Ovalbumin (product A5503, purity 98% according to agarose gel electrophoresis) and linoleic acid (LA) samples were purchased from Sigma (USA). LA sample was kept under N_2 atmosphere at −18 °C according to manufacturer advices. Fluorescence probe 1-anilino-8-naphthalene sulfonic acid (ANS) was obtained from Fluka Chemie AG (Switzerland).

2.2. Preparation and characterization of protein samples

2.2.1. Formation of OVA nanoparticles

OVA solutions 10 g/L were prepared in 50 mM NaCl and were kept overnight at 4 °C. Then, pH was adjusted at 7.5 using NaOH and solutions were filtered with 0.22 μm cellulose ester membranes (Millipore) in order to eliminate possible protein aggregates. Protein concentration was verified from the absorption at 280 nm using an OVA extinction coefficient of 0.712 $L\,g^{-1}\,cm^{-1}$ [4].

For heat treatment, the temperature range was chosen around OVA denaturation temperature (80.1 °C) [19] in order to study the extent to which the buried hydrophobic residues expose. OVA solutions were heated in a water bath at 75, 80 and 85 °C. These systems were called OVA-75, OVA-80 and OVA-85, respectively. Stoppered glass tubes were removed from the water bath at different times (3, 5, 10, 15, 20, 25 min), and immediately were cooled in an ice bath. Subsequently, samples were kept at 4 °C until further analysis. Environmental conditions (pH 7.5 and ionic strength 50 mM NaCl) under which heat treatment was performed were fixed in order to allow high electrostatic repulsion and, consequently, low aggregation.

2.2.2. Particle size distribution analysis of native OVA and nanoparticles

Particle size distribution (PSD) was obtained by dynamic light scattering (DLS) at a set angle of 90 °C, using a Zetasizer Nano ZS90 – Malvern Instruments Ltd., UK. The instrument is equipped with a He–Ne laser at a wavelength output of 632.8 nm. Samples were diluted at a convenient concentration according to instrument quality parameters. The refractive indexes for solvent and protein aggregates used were 1.33 and 1.50, respectively [4]. The mean hydrodynamic diameter was obtained from the peak of intensity *versus* diameter (nm) curve. Polydispersity index (PdI) was also considered in PSD analysis [20]. Measurements were made at 25 °C and were performed in duplicate.

2.2.3. Extrinsic fluorescence of native OVA and nanoparticles

Extrinsic fluorescence spectra were obtained using a Hitachi F-2000 fluorescence spectrophotometer (Japan). For this, 10 μl of 8 mM ANS solution was added to 2 ml of 0.043 g/L protein dispersion. These protein dispersions were prepared re-dispersing aliquots from native and heated samples in 50 mM pH 7 phosphate buffer. Emission spectra were registered between 450 and 550 nm, at λ_{ex} = 390 nm [4]. For each spectrum, the maximum fluorescence intensity (FI-ANS) and its wavelength (λ_{ANS}) were registered. Fluorescence intensities results were informed as ANS relative fluorescence intensity (RFI-ANS) which was defined as the ratio between FI-ANS of heat-treated solution to FI-ANS of native OVA solution. RFI-ANS was taken as a measure of protein surface hydrophobicity. On the other hand, shifts of λ_{ANS} were reported as $\Delta\lambda$ which was calculates as the difference between heat-treated OVA λ_{ANS} and native OVA λ_{ANS}. Extrinsic fluorescence experiments were performed in triplicate at room temperature [12].

2.3. Binding properties of OVA and nanoparticles

The LA binding properties of OVA and nanoparticles were studied by mean of intrinsic and extrinsic fluorescence, turbidity, particles size distributions and ζ-potential measurements. LA/OVA nanocomplexes were prepared by mixing OVA samples with LA as will be described bellow.

2.3.1. Fluorescence measurements

Intrinsic fluorescence (due to Trp emission) of native OVA, OVA-75, OVA-80 and OVA-85 heated for 5 and 25 min was determined using a Hitachi F-2000 fluorescence spectrophotometer (Japan). OVA solutions were diluted in 50 mM pH 7 phosphate buffer in order to obtain a final protein concentration of 0.043 g/L. Then, 2 ml of protein solution were manually titrated with increasing volumes (0–10 μl using a micropipette) of 15 mM LA in ethanolic solution. Final ethanol concentration was lower than 0.5% (v/v) and had no effect on the fluorescence experiment [15]. In order to allow equilibration, resultant solutions were kept for 3 h previous to fluorescence measurement. Emission spectra were obtained between 310 and 360 nm exciting at λ_{ex} = 280 nm. From each spectrum, maximum emission fluorescence intensity (FI) was registered. Results were informed as relative fluorescence intensity (RFI) which was calculated as ratio between the FI at a given LA concentration and FI at zero LA concentration. Titration curves were represented as RFI *versus* LA concentration [13]. Measurement was carried out in triplicate at room temperature.

The association constants (K_A) might be considered as an estimation of the LA binding ability of OVA and will be obtained as follow:

$$K_A = \frac{[FQ]}{[F]\cdot[Q]} \quad (1)$$

where [*FQ*] is the concentration of the complex, [*F*] is the concentration of uncomplexed fluorophore, and [*Q*] is the concentration

of quencher (LA). Hence, total fluorophore concentration is given by:

$$[F_0] = [F] + [FQ] \quad (2)$$

Substituting Eq. (2) into Eq. (1) and rearranging:

$$K_A = \frac{[F_0] - [F]}{[F] \cdot [Q]} = \frac{[F_0]}{[F] \cdot [Q]} - \frac{1}{[Q]} \Rightarrow \frac{[F_0]}{[F]} = K_A \cdot [Q] + 1 \quad (3)$$

Fluorophore concentration can be substituted by fluorescence intensities:

$$\frac{F_0}{F} = K_A \cdot [Q] + 1 \quad (4)$$

where F_0 and F are fluorescence intensities without and with LA, respectively. Eq. (4) shows the linear dependence of F_0/F on [Q] and K_A can be calculated as the slope of F_0/F *versus* [Q] [28]. Hence, the sample with the highest K_A and so the highest LA binding ability will be used for the study of further binding properties.

On the other hand, extrinsic fluorescence spectrum was obtained. Samples were prepared adding 10 μl of 8 mM ANS solution to 2 ml of solution containing 0.043 g/L OVA aggregates (obtained at 85 °C, 5 min) and 70 μM of LA. Then, the emission spectrum (410–530 nm) was obtained exciting at 390 nm. Measurement was carried out in triplicate at room temperature.

2.3.2. Turbidity measurement

For turbidity measurement, increasing volumes (0–10 μl) of 100 mM LA in ethanolic solution were manually added to 2 ml of native OVA and OVA-85 treated for 5 min (OVA-85,5) solutions. Protein concentration was 0.5 g/L in 50 mM pH 7 potassium phosphate buffer. A system without protein was also prepared. Then, absorbance at 400 nm was measured as an index of turbidity [17]. Measurements were performed in triplicate using a Jenway 7305 spectrophotometer (UK).

2.3.3. Particle size distribution analysis and ζ-potential measurement

PSD analysis of OVA-85,5 (2 g/L in phosphate buffer 50 mM pH 7) with and without 1 mM LA were carried out as it was described in Section 2.2.2. Also, 1 mM LA solution was measured. Measurements were performed in triplicate at 25 °C.

ζ-Potential measurements of OVA-85,5 (2 g/L in phosphate buffer 50 mM pH 7) with and without 1 mM LA were performed using a Zetasizer Nano ZS90 – Malvern Instruments Ltd., UK. The instrument determinates the distribution of the electrophoretic mobility of nanoparticles by mean of the laser Doppler velocity technique. The ζ-potential value was calculated according to Smoluchowski model using the software that equipment provides. Measurements were performed in triplicate at 25 °C.

3. Results

3.1. Characterization of native OVA and nanoparticles

3.1.1. Particle size distribution analysis of native OVA and nanoparticles

Intensity of scattered light *versus* particle size (PSD) of native and heat-treated OVA solutions are displayed in Fig. 1. Samples present monomodal PSDs, so the intensity peak of PSD is taken as the mean hydrodynamic diameter [20]. The hydrodynamic diameter is the diameter of an equivalent sphere that diffuses at the same average rate as the particle under examination [21]. It can be seen that OVA-75 present wider size distributions than OVA-80 and OVA-85. Moreover, PdI values of OVA-75 (0.25–0.28) are greater than OVA-80 and OVA-85 (0.19–0.20 and 0.20–0.22, respectively). It is important to highlight that PdI values close to 0.05 indicate highly

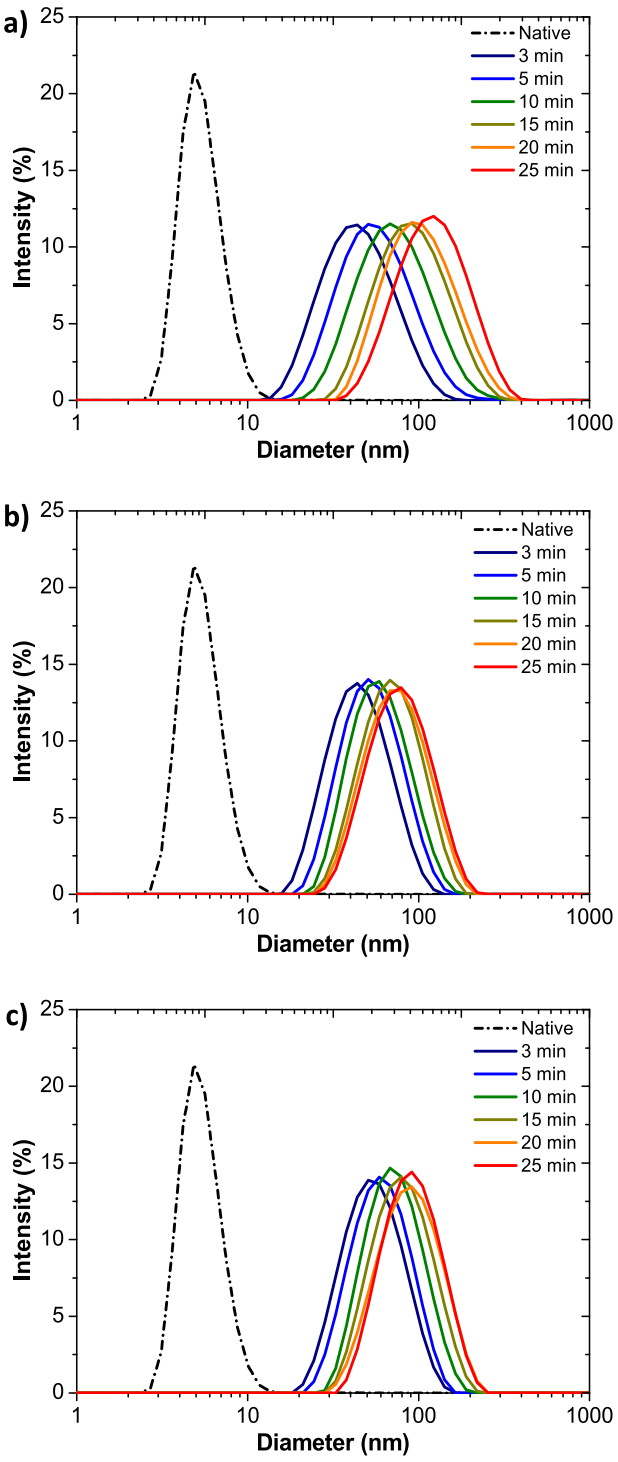

Fig. 1. Intensity PSD of heat-treated OVA at: (a) 75 °C, (b) 80 °C and (c) 85 °C for 0, 3, 5, 10, 15, 20 and 25 min.

monodispersed PSDs while PdI values greater than 0.7 corresponds to polydispersed PSDs [34]. Furthermore, PSDs for the different heating times, were closer for OVA-80 and OVA-85 than OVA-75. Fig. 2 shows the mean hydrodynamic diameter *versus* heating time for 75, 80 and 85 °C. The aggregates sizes are around 100 nm, so that OVA aggregates could be considered as "OVA nanoparticles" (OVA_n) [22]. It can be seen that, for the three heat treatments, mean OVA_n diameter increase with heating time until reach a *plateau*. OVA_n sizes obtained at the different conditions are comparable to the ones obtained by Croguennec et al. [4], who worked in

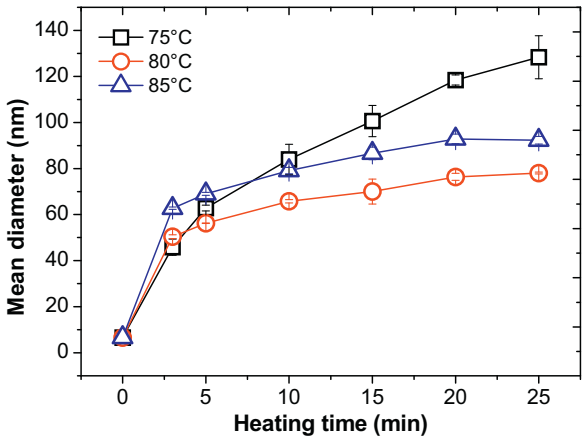

Fig. 2. Mean diameter for different heating time and temperature. Error bars are the standard deviation of the duplicate analyses.

similar conditions (80 °C, pH 7, 50 mM NaCl, 10 g/L OVA). As shown in Fig. 2, OVA_n size increase with heating temperature for a heating time of 3 min. These aggregates would be formed mainly by mean of hydrophobic interactions which govern initial stages of protein aggregation [23]. During heat treatment, in first place, a partial unfolding/denaturation of OVA is produced, so that buried hydrophobic regions into globular structure become exposed to aqueous medium [2]. Then, the initially formed aggregates (stabilized by hydrophobic interactions) would be stiffened through disulfide bridge formation. This covalent bound would take place at long heating time [23]. As also can be seen in Fig. 2, nanoparticle mean diameter of treated OVA after 10 min presented the following order: OVA-75 > OVA-85 > OVA-80. The largest size in OVA-75 could be explained taking into account that hydrophobic attractions increase as temperature is raised up to 60–70 °C and above this temperature start to decrease [24]. Hence, hydrophobic attractions would be more favored at 75 °C than 80 and 85 °C. Consequently, more aggregation *via* hydrophobic attractions would take place at 75 °C giving larger size of OVA-75 nanoparticles than OVA-80 and OVA-85 ones.

3.1.2. Extrinsic fluorescence of native OVA and nanoparticles

Heat treatments of protein solutions induce denaturation of protein with the consequent unfolding of the molecular structure and exposition of the buried hydrophobic regions. This phenomenon confers a greater surface hydrophobicity to the protein. Surface hydrophobicity can be determinated by mean of extrinsic fluorescence measurements using the probe 1-anilino-8-naphthalene sulfonic acid (ANS) [4,19]. The interaction of ANS with protein hydrophobic areas is normally characterized by a considerable rise in ANS fluorescence intensity in comparison to weak ANS fluorescence observed in water. Besides, shifts in maximum emission intensity towards lower wavelength values (blue shift) are registered [25]. It is known that extension of denaturation and, consequently, extrinsic fluorescence intensity increase sharply when OVA solution is heated above 70 °C [6]. Regarding to extrinsic fluorescence intensity, Fig. 3a shows that heat treatment produced an increase of 6–8 folds in RFI-ANS values of OVA respect to the native OVA. RFI-ANS values of OVA-75 significantly ($p < 0.05$) increase with heating time, while RFI-ANS values of OVA-80 and OVA-85 reach a maximum value at 5 min. The highest surface hydrophobicity was recorded for OVA-80 and OVA-85 at 5 min and for OVA-80 at 25 min.

On the other hand, in heat-treated OVA spectra, wavelength blue shifts were registered for ANS maximum emission. These results are shown in Fig. 3b where $\Delta\lambda$ (blue shift) is the difference between λ_{ANS} of native OVA and heat-treated OVA. A similar behavior to that of RFI-ANS is observed. $\Delta\lambda$ of OVA-75, increased with heating time, while $\Delta\lambda$ of OVA-80 and OVA-85 reach a maximum at 5 min. The maximum shift value is found for OVA-80.

The RFI-ANS and $\Delta\lambda$ results would mean that OVA exposed the buried hydrophobic regions during heat treatment and so these regions become more accessible to ANS. The blue shift indicates that ANS molecules would be in a more hydrophobic environment [25]. The behavior of OVA-80 and OVA-85, could suggested that the majority of OVA molecules were already denatured/unfolded at 5 min heating and further heating did not induce an additional denaturation. These results are according with Croguennec et al. [4]. On the other hand, OVA-75 did not present this behavior, indicating that protein denaturation could not be completed after 5 min heating.

3.2. Binding properties of OVA and nanoparticles

3.2.1. Fluorescence measurements

Intrinsic fluorescence can be used to study binding properties of proteins [26]. OVA have three fluorescent aminoacids residues: tryptophan (Trp), tyrosine (Tyr) and phenylalanine (Phe). However, Trp is the fluorescence dominant residue, due to take place energy transference from Tyr and Phe to Trp [15]. At $\lambda_{ex} = 280$ nm, both Tyr and Trp residues are excited [26]. One OVA molecule possesses three Trp residues: Trp148 on the F helix, Trp267 on H helix and Trp184 near to 3A carboxyl extreme [14,27]. When proteins and their aggregates bind to ligands, their intrinsic fluorescence can decrease which is known as fluorescence quenching [14,26]. Non-fluorescent ground-state complexes absorb light and they returns immediately to ground state without photon emission [28].

In the present work, RFI *versus* LA concentration curves for OVA-75, OVA-80, OVA-85 at 5 and 25 min of heating and native OVA as a control were obtained. These samples were selected because it was

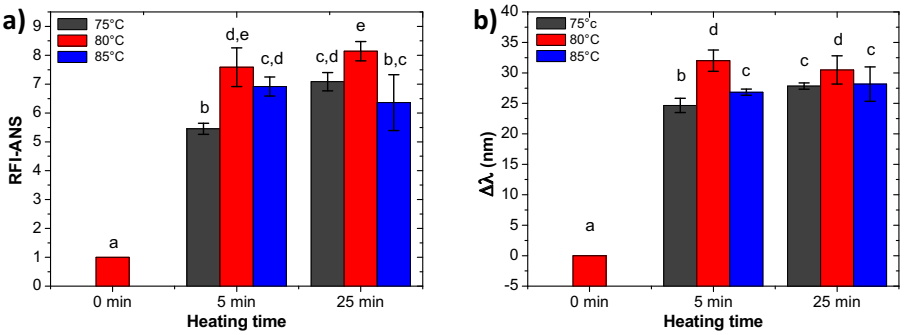

Fig. 3. Extrinsic fluorescence of native and heat-treated OVA (75, 80 and 85 °C). a) Relative Fluorescence Intensity (RFI-ANS). (b) Wavelength blue shift ($\Delta\lambda$). Different letters indicate a significant difference ($p < 0.05$).

Please cite this article in press as: O.E. Sponton, et al., Linoleic acid binding properties of ovalbumin nanoparticles, Colloids Surf. B: Biointerfaces (2015), http://dx.doi.org/10.1016/j.colsurfb.2015.01.037

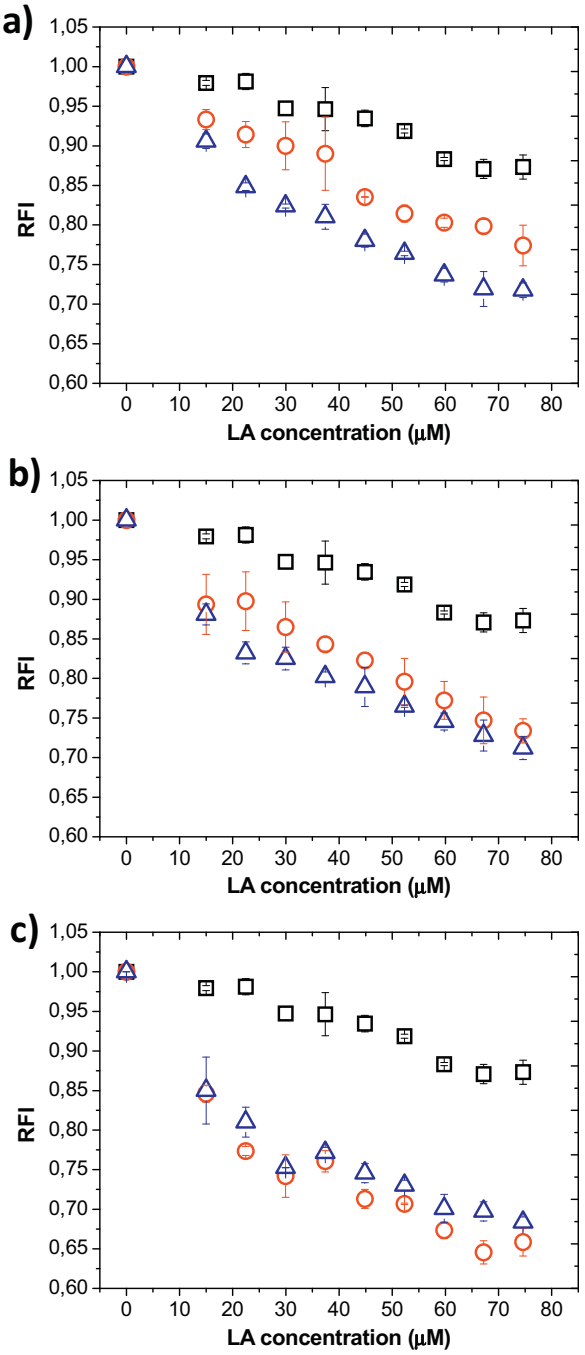

Fig. 4. Relative fluorescence Intensity as function of LA concentration for heat-treated OVA at (a) 75 °C, (b) 80 °C and (c) 85 °C for 0 min ( ), 5 min ( ) and 25 min ( ). Protein concentration: 0.043 g/L.

previously demonstrated that heating of OVA solution (pH 7, 80 °C, NaCl 50 mM) reached the maximum surface hydrophobicity after 5 min of treatment. Further heating only produced aggregation and not additional unfolding (exposition of buried hydrophobic residues) [4]. Hence, samples heated at 5 min might be suitable to bind LA molecules due to the high surface hydrophobicity and lower size. Meanwhile, OVA_n obtained at 25 min was studied in order to analyze what happen with the surface hydrophobicity and binding ability, at long term heat treatment. Fig. 4(a–c) displays RFI *versus* LA concentration for OVA-75, OVA-80, OVA-85 at 5 and 25 min and native OVA as a control. These curves are analyzed taking into account that quenching magnitude (RFI decrease)

Table 1
K_A values [M^{-1}] (mean ± standard deviation) for native OVA and heat-induced OVA nanoparticles.

Sample	Heating time	
	5 min	25 min
OVA-75	3578 ± 774^{b}	5275 ± 222^{cd}
OVA-80	4842 ± 136^{c}	4979 ± 318^{cd}
OVA-85	6659 ± 264^{e}	5604 ± 143^{d}
Native OVA	2192 ± 120^{a}	

Different letters indicate a significant difference ($p < 0.05$).

is proportional to protein–LA complex concentration [14,28]. As can be seen in Fig. 4, RFI of native OVA shows a low decrease with the increase in LA concentration hence slight fluorescence quenching, while RFI of OVA_n decrease more abruptly indicating a greater quenching phenomenon with temperature increment. OVA-75,25 (Fig. 4a) show higher OVA-LA complex formation than OVA-75,5. A similar tendency was observed for OVA-80 (Fig. 4b), although curves for 5 and 25 min were closer. In OVA-85 (Fig. 4c), this tendency was inverted, suggesting a slight higher complex formation for OVA-85,5 than OVA-85,25.

On the other hand, for all heat-treated OVA, a significant blue shift of 2 nm ($p < 0.05$) in the wavelength of maximum fluorescence intensity was registered (data no shown). Blue shifts in the wavelength indicate a more apolar environment of Trp residues. This result could be explained taking into account that LA is an amphiphilic molecule which has a small polar head (an ionized carboxyl group) and a long hydrophobic tail (an aliphatic chain) [30]. Thus, Trp residues in presence of LA would be in a more apolar environment [28], probably due to the closeness to LA hydrophobic tail. This behavior was not observed in native OVA, which showed no change in the wavelength of the fluorescence intensity maximum, indicating that Trp would not be involved in the union of LA to native OVA. About this, Kamilya et al. [15] studied native OVA-stearic acid interaction and they proposed that Tyr residue would be a probable binding site for fatty acid. The carboxylic extreme of stearic acid would perturb Tyr excitation and, consequently, Trp fluorescence quenching. Stearic acid incorporation would not allow energy transfer from Tyr to Trp.

Fluorescence quenching can be described for Eq. (4). When F_0/F *versus* [Q] is effectively linear, there is a single class of fluorophore, all equally accessible to the quencher [26,28]. The K_A value is indicative of complex concentration and surface exposition of fluorophore to ligand or quencher [28]. In the present work, all binding assays were fitted according to Eq. (4), with R^2 between 0.863 and 0.987. Table 1 presents K_A values [M^{-1}]. It can be noted that native OVA shows the lowest K_A value, suggesting that native OVA has lower LA binding ability than OVA_n. OVA-75 shows an increase in K_A value with heating time, while OVA-85 exhibits an opposite tendency being K_A value at 5 min higher than the one at 25 min of heating. On the other hand, OVA-80 does not present significant difference ($p < 0.05$) for K_A value with heating time.

Comparing K_A of OVA_n with the surface hydrophobicity for 25 min of heat-treatment, it was found that the maximum value of surface hydrophobicity (OVA-80) did not correspond with the maximum K_A value. It is important to remark that both, OVA-80 and OVA-85 present the maximum surface hydrophobicity for 5 min of heat-treatment (Fig. 3), but only OVA-85 shows the maximum K_A (Table 1). Hence, the ability of OVA_n to bind LA would depend not only on surface hydrophobicity, but also would depend on protein structure, *i.e.*, the formation of hydrophobic sites at the surface or in the inner structure of the aggregates, capable to accommodate LA molecules [11].

Fig. 5 displays ANS emission spectra of OVA_n (OVA-85,5) with and without LA. As it can be noted, the presence of LA produce

Please cite this article in press as: O.E. Sponton, et al., Linoleic acid binding properties of ovalbumin nanoparticles, Colloids Surf. B: Biointerfaces (2015), http://dx.doi.org/10.1016/j.colsurfb.2015.01.037

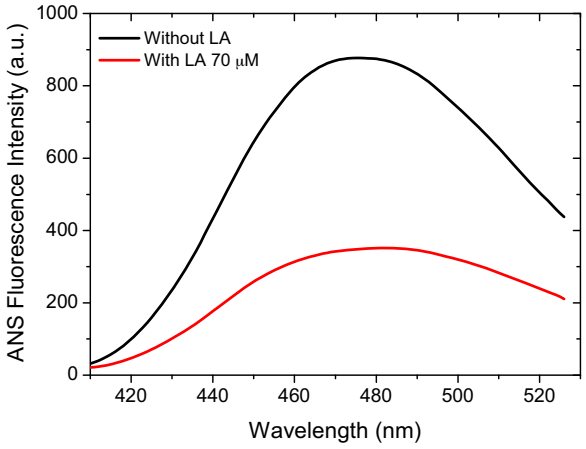

Fig. 5. ANS emission fluorescence spectrum of OVA nanoparticles with and without LA. Protein concentration: 0.043 g/L.

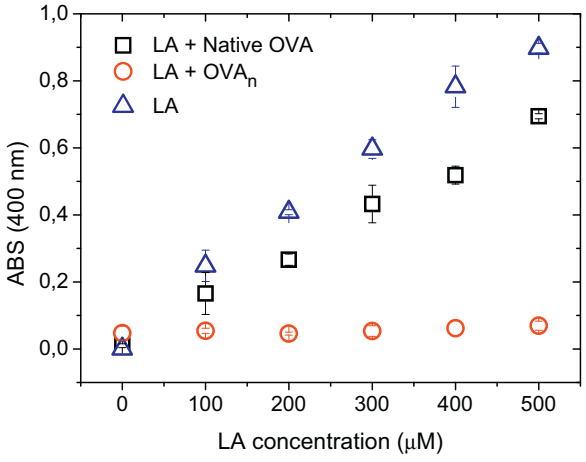

Fig. 6. Absorption at 400 nm *versus* LA concentration system without protein and with native OVA and OVA nanoparticles (OVA-85,5). Protein concentration: 0.5 g/L.

a decrease of 2.5 folds in the maximum intensity of ANS fluorescence (from 877 ± 10 to 352 ± 25 nm for solutions without and with LA, respectively). Furthermore, a red shift in the maximum wavelength (from 476 ± 0 to 483 ± 1 nm for solution without and with LA, respectively) was registered. This result could indicate that minor ANS fraction is bound to the hydrophobic sites on the protein because they might be occupied by LA molecules [29]. Besides, these facts are coherent with the blue shift of 2 nm in the wavelength of intrinsic fluorescence intensity and they would indicate that the union of LA to OVA_n would be by mean of hydrophobic interactions.

3.2.2. Turbidity measurement

As it was mentioned, a PUFA molecule is an amphiphilic molecule which has a small polar head (an ionized carboxyl group) and a long hydrophobic tail (an aliphatic chain) [30]. The latter confers them high hydrophobicity and, consequently, very low water solubility [9]. In an aqueous solution, when PUFA concentration exceeds a critical value, known as the *critical micelle concentration* (CMC), supramolecular self-assembly of fatty acids appear, forming big micelles and vesicles, which confer turbidity to the solution [17,31]. This phenomenon occurs because fatty acid molecules associate with tails close to each other while heads remain in contact with water molecules [30]. At pH 7.6 and room temperature, solubility reaches a maximum around 60 μM which correspond to CMC [9]. Fig. 6 shows that turbidity, measured as absorption at

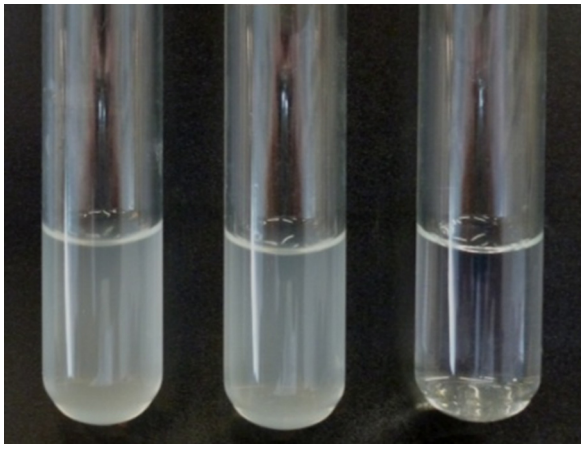

Fig. 7. Visual appearance of 500 μM LA solutions, without OVA (left), with native OVA (center) and with OVA-85,5 nanoparticles (right). Protein concentration: 0.5 g/L.

400 nm, increased linearly with LA concentration (in 50 mM pH 7 phosphate buffer without protein). These solutions present turbidity because the sizes of LA supramolecular self-assemblies are on the same order of light wavelength. Hence, strong light scattering take place [18]. However, when LA is added in a OVA_n (OVA-85,5) solution, turbidity decrease and solution tends to be transparent. This result could suggest the disruption of LA supramolecular self-assemblies and the formation of OVA_n–LA nanocomplexes due to LA bind to OVA_n [17]. Under the same conditions, native OVA produced a slight decrease in turbidity which would indicate that LA molecules bind to native OVA in a low concentration. This result is consistent with the lowest binding ability determined from fluorescence measurements, discussed in Section 3.2.1.

Fig. 7 shows the visual appearance of 500 μM LA solution without OVA (left), with native OVA (center) and with OVA-85,5 (right). As can be seen, OVA-85,5 produced a visible decrease in LA solution turbidity reaching an almost transparent appearance. A transparent or slightly turbid solution indicates that the size of dispersed particles is smaller than the light wavelength producing a relatively weak light scattering [18]. According to this result, OVA-85,5 could be proposed for the development OVA_n to vehiculizate PUFAs. Although nanometric materials are stable to gravitational separation because Brownian motion predominates against gravitational forces [18], stability studies under different conditions (pH, ionic strength, temperature, *etc.*) are necessary in order to verify nanoparticles stability.

3.2.3. Particle size distribution analysis and ζ-potential measurement

Fig. 8 shows PSDs of OVA_n (OVA-85,5), OVA_n–LA complexes and LA supramolecular self-assemblies. It can be noted that LA PSD presented a peak of 611 ± 8 nm which was not found in the presence of OVA_n. These results would indicate the disruption of LA micelles and would confirm OVA_n–LA nanocomplexes formation as it was discussed in Section 3.2.2 [17]. Moreover, it can be seen that OVA_n–LA PSD is very close to OVA_n PSD. However, the OVA_n–LA PSD presented a mean diameter of 87.5 ± 1.2 nm which was significantly larger than OVA_n mean diameter (79.4 ± 1.8 nm). The larger size of OVA_n–LA could be explained by LA deposition onto the surface of OVA_n giving an increase in hydrodynamic diameter.

On the other hand, ζ-potential measurements were also carried out. The electric potential at the shear plane between the bound layer of ions surrounding a particle and the bulk solution is known as ζ-potential [32]. The bound layer of ions is composed by two parts: (i) the Stern layer, where the ions are strongly bound on the

Please cite this article in press as: O.E. Sponton, et al., Linoleic acid binding properties of ovalbumin nanoparticles, Colloids Surf. B: Biointerfaces (2015), http://dx.doi.org/10.1016/j.colsurfb.2015.01.037

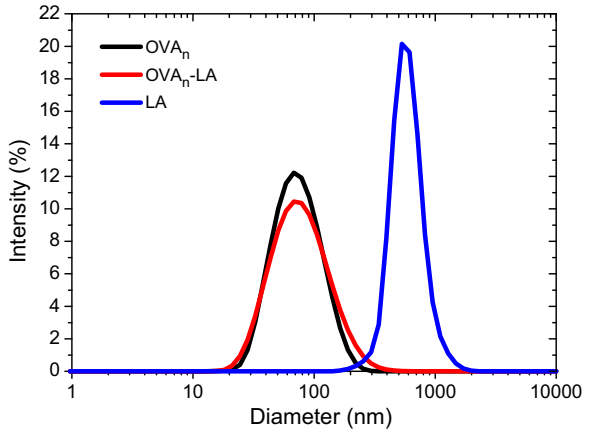

Fig. 8. Intensity PSD of OVA nanoparticles (OVA-85,5) solution with and without LA 1 mM. Protein concentration: 2 g/L. A system without protein was also included.

particle and (ii) the diffuse layer where ions are less firmly associated. The ζ-potential can be modified by adsorption of charged species such as ions and ionic surfactants on particle surface [33]. In this work, ζ-potential measurements at pH 7 (phosphate buffer 50 mM) of OVA_n (OVA-85,5) and OVA_n–LA complexes were carried out. Results show that OVA_n–LA complexes presented significant ($p < 0.05$) lower ζ-potential value than OVA_n one (-14.8 ± 0.4 mV and -18.6 ± 0.9 mV, respectively). As was mentioned, LA molecule has an apolar tail (aliphatic chain) and a polar head (carboxylic group) conferring it an amphiphilic character. Hence, if LA is bound to OVA_n by mean of hydrophobic interactions through apolar tail, the ionized polar head would be oriented to the nanocomplex surface in contact with aqueous medium increasing the negative charge of OVA_n. This result is according to the ones obtained in Section 3.2.2.

4. Conclusions

In the present work, it was demonstrated that ovalbumin nanoparticles with LA binding properties can be obtained by heat treatment. These nanoparticles presented higher surface hydrophobicity and higher LA binding ability than native OVA. From fluorescence and ζ-potential analysis it could be deduced that LA binds to OVA_n by mean of hydrophobic interactions. Moreover, it is important to remark that OVA_n (OVA-85,5) produced clear solutions due to OVA_n–LA nanocomplexes formation. The ability of OVA_n to form nanocomplexes with LA could allow the development of PUFAs nanovehicles with potential application in several industrial sectors. However, not only stability under different conditions but also PUFAs release studies is necessary in order to check the nanoparticles aptitude to incorporate them in foods.

Acknowledgements

We acknowledge the financial support of project CAI+D PI–2011 501 201 101 00 171 LI (UNL, Santa Fe, Argentina). Authors would like to thank Consejo Nacional de Investigaciones Científicas y Técnicas de la República Argentina (CONICET) for the fellowships awarded to Osvaldo E. Sponton.

References

[1] K. Nyemb, C. Guérin-Dubiard, D. Dupont, J. Jardin, S.M. Rutherfurd, F. Nau, The extent of ovalbumin in vitro digestion and the nature of generated peptides are modulated by the morphology of protein aggregates, Food Chem. 157 (2014) 429–438.
[2] M. Weijers, L.M.C. Sagis, C. Veerman, B. Sperber, E. van der Linden, Rheology and structure of ovalbumin gels at low pH and low ionic strength, Food Hydrocoll. 16 (3) (2002) 269–276.
[3] C.V.L. Giosafatto, N.M. Rigby, N. Wellner, M. Ridout, F. Husband, A.R. Mackie, Microbial transglutaminase-mediated modification of ovalbumin, Food Hydrocoll. 26 (2012) 261–267.
[4] T. Croguennec, A. Renault, S. Beaufils, J. Dubois, S. Pezennec, Interfacial properties of heat-treated ovalbumin, J. Colloid Interface Sci. 315 (2007) 627–636.
[5] A. Kato, Y. Nagase, N. Matsudomi, K. Kobayashi, Determination of molecular weight of soluble ovalbumin aggregates during heat denaturation using low laser light scattering technique, Agric. Biol. Chem. 47 (8) (1983) 1829–1834.
[6] V.B. Galazka, D. Smith, D.A. Ledward, E. Dickinson, Interactions of ovalbumin with sulphated polysaccharides: effects of pH, ionic strength, heat and high pressure treatment, Food Hydrocoll. 13 (1999) 81–88.
[7] M. Weijers, P.A. Barneveld, M.A. Cohen Stuart, R.W. Visschers, Heat-induced denaturation and aggregation of ovalbumin at neutral pH described by irreversible first-order kinetics, Protein Sci. 12 (2003) 2693–2703.
[8] M. Weijers, K. Broersen, P.A. Barneveld, M.A. Cohen Stuart, R.J. Hamer, H.H.J. De Jongh, R.W. Visschers, Net charge affects morphology and visual properties of ovalbumin aggregates, Biomacromolecules 9 (2008) 3165–3172.
[9] P. Zimet, Y.D. Livney, Beta-lactoglobulin and its nanocomplexes with pectin as vehicles for ω-3 polyunsaturated fatty acids, Food Hydrocoll. 23 (2009) 1120–1126.
[10] S.A. Fioramonti, A.A. Perez, E.E. Aríngoli, A.C. Rubiolo, L.G. Santiago, Design and characterization of soluble biopolymer complexes produced by electrostatic self-assembly of a whey protein isolate and sodium alginate, Food Hydrocoll. 35 (2014) 129–136.
[11] S. Le Maux, S. Bouhallab, L. Giblin, A. Brodkorb, T. Croguennec, Complexes between linoleate and native or aggregated β-lactoglobulin: interaction parameters and in vitro cytotoxic effect, Food Chem. 141 (2013) 2305–2313.
[12] A.A. Perez, R.B. Andermatten, A.C. Rubiolo, L.G. Santiago, β-Lactoglobulin heat-induced aggregates as carriers of polyunsaturated fatty acids, Food Chem. 158 (2014) 66–72.
[13] O.E. Sponton, A.A. Perez, C. Carrara, L.G. Santiago, Effect of limited enzymatic hydrolysis on linoleic acid binding properties of β-lactoglobulin, Food Chem. 146 (2014) 577–582.
[14] R. Wang, Y. Yin, H. Li, Y. Wang, J. Pu, R. Wang, et al., Comparative study of the interactions between ovalbumin and three alkaloids by spectrofluorimetry, Mol. Biol. Rep. 40 (2013) 3409–3418.
[15] T. Kamilya, P. Pal, G.B. Talapatra, Interaction and incorporation of ovalbumin with stearic acid monolayer: Langmuir–Blodgett film formation and deposition, Colloids Surf. B 58 (2007) 137–144.
[16] H. Ilyasoglu, S.H. El, Nanoencapsulation of EPA/DHA with sodium caseinate–gum arabic complex and its usage in the enrichment of fruit juice, Food Sci. Technol. 56 (2014) 461–468.
[17] A. Fontana, B. Spolaore, P. Polverino de Laureto, The biological activities of protein/oleic acid complexes reside in the fatty acid, Biochim. Biophys. Acta 1834 (2013) 1125–1143.
[18] D.J. McClements, Y. Li, Structured emulsion-based delivery systems: controlling the digestion and release of lipophilic food components, Adv. Colloid Interface Sci. 159 (2010) 213–228.
[19] N. Matsudomi, H. Takahashi, T. Miyata, Some structural properties of ovalbumin heated at 80 °C in the dry state, Food Res. Int. 34 (2–3) (2001) 229–235.
[20] F.A.O. Carvalho, J.W.P. Carvalho, F.R. Alves, M. Tabak, pH effect upon HbGp oligomeric stability: characterization of the dissociated species by AUC and DLS studies, Int. J. Biol. Macromol. 59 (2013) 333–341.
[21] Niidome, Application note: The Use of Light Scattering to Study the Structure and charge of Dendritic Poly(L-Lysine), 2014 http://www.malvern.com/en/pdf/secure/AN101104ChargeDendritic_Poly_L_Lysine_.pdf (accessed 11.12.14).
[22] F.J. Gutiérrez, S.M. Albillos, E. Casas-Sanz, Z. Cruz, C. García-Estrada, A. García-Guerra, et al., Methods for the nanoencapsulation of β-carotene in the food sector, Trends Food Sci. Technol. 32 (2013) 73–83.
[23] A.C. Sánchez-Gimeno, A.V.P. López-Buesa, Studies of ovalbumin gelation in the presence of carrageenans and after manothermosonication treatments, Innov. Food Sci. Emerg. Technol. 7 (2006) 270–274.
[24] C.M. Bryant, D.J. McClements, Molecular basis of protein functionality with special consideration of cold-set gels derived from heat-denatured whey, Trends Food Sci. Technol. 9 (1998) 143–151.
[25] J.R. Albani, Structure a Dynamics of Macromolecules: Absorption and Fluorescence Studies, Elsevier, Paris, 2004 (Chapters 2 & 3).
[26] A. Shpigelman, G. Israeli, Y. Livney, Thermally-induced protein-polyphenol co-assemblies: beta lactoglobulin-based nanocomplexes as protective nanovehicles for EGCG, Food Hydrocoll. 24 (2010) 735–743.
[27] V. Lechevalier, T. Croguennec, S. Pezennec, C. Guérin-Dubiard, M. Pasco, F. Nau, Evidence for synergy in the denaturation at the air–water interface of ovalbumin, ovotransferrin and lysozyme in ternary mixture, Food Chem. 92 (2005) 79–87.
[28] J.R. Lakowicz, Principles of Fluorescence Spectroscopy, 3rd ed., Springer, Singapore/USA, 2006 (Chapter 8).
[29] W.G. Gonzalez, J. Miksovska, Application of ANS fluorescent probes to identify hydrophobic sites on the surface of DREAM, Biochim. Biophys. Acta 1844 (2014) 1472–1480.
[30] O.R. Fennema, Food Chemistry, 3rd ed., Marcel Dekker Inc., New York, 1996 (Chapter 3).

[31] C.C. Akoh, D.B. Min, Food Lipids. Chemistry, Nutrition, and Biotechnology, 2nd ed., Marcel Dekker Inc., New York, 2002 (Chapter 3).
[32] Malvern Instruments Limited, Zeta Potential Analysis using Z-NTA (Zeta Potential Nanoparticle Tracking Analysis), 2014 http://www.malvern.com/en/pdf/secure/TN140827ZetaPotentialAnalysisUsingZNTA.pdf (accessed 11.12.14).
[33] Malvern Instruments Limited, Zeta potential – An introduction in 30 minutes, 2014 http://www.malvern.com/en/pdf/secure/TN101104ZetaPotentialIntroduction.pdf (accessed 11.12.14).
[34] Malvern Instruments Limited, Dynamic light scattering – common terms defined, 2014 http://www.malvern.com/en/pdf/secure/WP111214DLSTermsDefined.pdf (accessed 10.12.14).

Please cite this article in press as: O.E. Sponton, et al., Linoleic acid binding properties of ovalbumin nanoparticles, Colloids Surf. B: Biointerfaces (2015), http://dx.doi.org/10.1016/j.colsurfb.2015.01.037